Throughput Analysis of Massive MIMO Uplink with Low-Resolution ADCs

Sven Jacobsson, *Student Member, IEEE,* Giuseppe Durisi, *Senior Member, IEEE,* Mikael Coldrey, *Member, IEEE,* Ulf Gustavsson, Christoph Studer, *Senior Member, IEEE*

Abstract

We investigate the information-theoretic throughput that is achievable over a frequency flat fading communication link when the receiver is equipped with low-resolution analog-to-digital converters (ADCs). We focus on the case where neither the transmitter nor the receiver have any *a priori* channel state information. This implies that the fading realizations have to be learned through pilot transmission followed by channel estimation at the receiver, based on coarsely quantized observations. We investigate the uplink throughput achievable by a massive multiple-input multiple-output system in which the base station is equipped with a large number of low-resolution ADCs. We propose a novel high-SNR approximation to the rate achievable with one-bit ADCs that is accurate for a broad range of system parameters. We show that for the one-bit quantized case, LS estimation together with maximal-ratio combing or zero-forcing detection enables reliable multi-user communication with high-order constellations in spite of the severe nonlinearity introduced by the ADCs. We demonstrate that the rate

S. Jacobsson is with Ericsson Research and Chalmers University of Technology, Gothenburg, Sweden (e-mail: sven.jacobsson@ericsson.com)

G. Durisi is with Chalmers University of Technology, Gothenburg, Sweden (e-mail: durisi@chalmers.se)

M. Coldrey and U. Gustavsson are with Ericsson Research, Gothenburg, Sweden (e-mail: {mikael.coldrey,ulf.gustavsson}@ericsson.com)

C. Studer is with Cornell University, Ithaca, NY (e-mail: studer@cornell.edu)

The work of S. Jacobsson and G. Durisi was supported in part by the Swedish Foundation for Strategic Research under grants SM13-0028 and ID14-0022, and by the Swedish Government Agency for Innovation Systems (VINNOVA) within the VINN Excellence center Chase.

The work of C. Studer was supported in part by Xilinx Inc., and by the US National Science Foundation (NSF) under grants ECCS-1408006 and CCF-1535897.

The material in this paper was presented in part at the IEEE International Conference on Communications (ICC) Workshop on 5G and Beyond: Enabling Technologies and Applications, London, U.K., June 2015 [1].

achievable in the infinite-precision (no quantization) case can be approached using ADCs with only a few bits of resolution. We finally investigate the robustness of the studied low-resolution ADC system against receive power imbalances between the different users, caused for example by imperfect power control.

Index Terms

Analog-to-digital converter (ADC), channel capacity, joint pilot-data (JPD) processing, least squares (LS) channel estimation, low-resolution quantization, multi-user massive multiple-input multiple-output (MIMO).

I. Introduction

Massive multiple-input multiple-output (MIMO) is a promising multi-user MIMO technology for next generation cellular communication systems (5G) [2]. With massive MIMO, the number of antennas at the base station (BS) is scaled up by several orders of magnitude compared to traditional multi-antenna systems with the goals of enabling significant gains in capacity and energy efficiency [2], [3]. Increasing the number of BS antenna elements leads to high spatial resolution; this makes it possible to simultaneously serve several user equipments (UEs) in the same time-frequency resource, which brings large capacity gains. The improvements in terms of radiated energy efficiency are enabled by the array gain that is provided by the large number of antennas.

Equipping the BS with a large number of antenna elements, however, considerably increases the hardware cost and the radio-frequency (RF) circuit power consumption [4]. This calls for the use of low-cost and power-efficient hardware components, which, however, reduce the signal quality due to an increased level of impairments. The aggregate impact of hardware impairments on massive MIMO systems has been investigated in, e.g., [5]–[7], where it is found that massive MIMO provides some degrees of robustness towards signal distortions caused by low-cost RF components.

A. Quantized Massive MIMO

In this paper, we consider an uplink massive MIMO system (i.e., UEs communicate to a BS) and focus on a particular source of signal distortion, namely the quantization noise caused by the use of low-resolution analog-to-digital converters (ADCs) at the BS. An ADC with sampling rate f_s Hz and a resolution of b bits maps each sample of the continuous-time, continuous-amplitude baseband received signal to one out of 2^b quantization labels, by operating $f_s \cdot 2^b$

conversion steps per second. In modern high-speed ADCs (e.g., with sampling rates larger than $1\,$GS/s), the dissipated power scales exponentially in the number of bits and linearly in the sampling rate [8], [9]. This implies that for wideband massive MIMO systems where hundreds of high-speed converters are required, the resolution of the ADCs may have to be kept low in order to maintain the power consumed at the BS within acceptable levels.

An additional motivation for reducing the ADC resolution is to limit the amount of data that has to be transferred over the link that connects the RF components and the baseband-processing unit. For example, consider a BS that is equipped with an antenna array of 500 elements. At each antenna element, the in-phase and quadrature samples are quantized separately using a pair of 10-bit ADCs operating at $1\,$GS/s. Such a system would produce 10 Tbit/s of data. This exceeds by far the rate supported by the common public radio interface (CPRI) used over today's fiber-optical fronthaul links [10]. Alleviating this capacity bottleneck is of particular importance in a cloud radio access network (C-RAN) architecture [11], where the baseband processing is migrated from the BSs to a centralized unit, which may be placed at a significant distance from the BS antenna array.

An implication of lowering the ADC resolution is that the requirement on accurate radio-frequency circuitry can be relaxed. The reason is that the quantization noise may be dominating the noise introduced by other components such as mixers, oscillators, filters, and low-noise amplifiers. Hence, further power-consumption reductions may be achieved by relaxing the quality requirements on the RF circuitry.

The one-bit resolution case, where the in-phase and quadrature components of the continuous-valued received samples are quantized separately using one-bit quantizers, is particularly attractive because of the resulting low hardware complexity [12], [13]. Indeed, a one-bit quantizer can be realized using only a simple comparator. Furthermore, in a one-bit architecture, there is no need for automatic gain control circuitry, which is otherwise needed to match the dynamic range of the ADCs.

B. Previous Work

Receivers employing low-resolution ADCs need to cope with the severe nonlinearity that is introduced by the coarse quantization, which may render signaling schemes and receiver algorithms developed for the case of high-resolution ADCs suboptimal.

The impact of the one-bit ADC nonlinearity on the performance of communication systems has been previously studied in the literature under various channel-model assumptions. In [14], it is proven that BPSK is capacity achieving over a real-valued nonfading single-input single-output (SISO) Gaussian channel. For the complex-valued Gaussian channel, QPSK is optimal.

These results hold under the assumption that the one-bit quantizer is a zero-threshold comparator. It turns out that in the low-SNR regime, a zero-threshold comparator is not optimal [15]. The optimal strategy involves the use of *flash-signaling* [16, Def. 2] and requires an optimization over the threshold value. Unfortunately, the power gain obtainable using this optimal strategy manifests itself only at extremely low values of spectral efficiency. Therefore, we shall focus exclusively on the zero-threshold comparator architecture in the remainder of the paper.

For the Rayleigh-fading case, under the assumption that the receiver has access to perfect channel state information (CSI), it is shown in [17] that QPSK is capacity achieving (again for the SISO case). The assumption that perfect CSI is available may, however, be unrealistic in the one-bit quantized case, since the nonlinear distortion caused by the one-bit quantizers makes channel estimation challenging. In particular, if the fading process evolves rapidly, the cost of transmitting training symbols cannot be neglected. For the more practically relevant case when the channel is not known *a priori* to the receiver, but must be learned (for example, via pilot symbols), QPSK is optimal when the SNR exceeds a certain threshold that depends on the coherence time of the fading process [18]. For SNR values that are below this threshold, on-off QPSK is capacity achieving [18].

For the one-bit quantized MIMO case, the capacity-achieving distribution is unknown. In [19], it is shown that QPSK is optimal at low SNR, again under the assumption of perfect CSI at the receiver. Mo and Heath Jr. [20] derived high-SNR bounds on capacity for the case when also the transmitter has access to perfect CSI.

The channel-estimation overhead in massive MIMO can be reduced using reciprocity-based time-division duplexing (TDD), where the channel estimates that have been obtained in the uplink are used for downlink beamforming [2]. Channel estimation on the basis of quantized observations is considered in, e.g., [21], [22] (see also [23] for a compressive-sensing version of this problem). A closed-form solution for the maximum likelihood (ML) estimate in the one-bit case is derived in [22], under the assumption of time-multiplexed pilots.

The use of one-bit ADCs in massive MIMO was considered in [24]. There, the authors examined the achievable uplink throughput for the scenario where the UEs transmit QPSK symbols, and the BS employs a least squares (LS) channel estimator, followed by a maximal ratio combining (MRC) or zero-forcing (ZF) detector. Their results show that large sum-rate throughputs can be achieved despite the coarse quantization. The results in [24] were extended to high-order modulations (e.g., 16-QAM) by the authors of this paper in [1]. There, we showed that one can detect not only the phase, but also the amplitude of the transmitted signal, provided that the number of BS antennas is sufficiently large and that the SNR is not too high. Choi *et al.* [25] recently developed a detector and a channel estimator capable of supporting high-order constellations such as 16-QAM.

A mixed-ADC architecture, where many one-bit ADCs are complemented with few high-precision ADCs on some of the antennas is proposed in [26]. It is found that the addition of a relatively small number of high-resolution ADCs increase the system performance significantly.

In all of the contributions reviewed so far, low-resolution quantized massive MIMO systems have been investigated solely for communication over frequency-flat, narrowband, channels. A spatial-modulation-based massive MIMO system over a frequency-selective channel was studied in [27]. The proposed receiver employs LS estimation followed by a message-passing-based detector. The performance of a low-resolution quantized massive MIMO system using orthogonal frequency division multiplexing (OFDM) and operating over a wideband channel was investigated in [28]. There, it is found that using ADCs with only four to six bits resolution is sufficient to achieve performance close to the infinite-precision (i.e., no quantization) case, at no additional cost in terms of digital signal processing complexity.

All of the results reviewed so far hold under the assumption of Nyquist-rate sampling at the receiver. However, it is worth pointing out that Nyquist-rate sampling is not optimal in the presence of quantization at the receiver [29], [30]. For example, for the one-bit quantized complex AWGN channel, high-order constellations such as 16-QAM can be supported even in the SISO case, if one allows for oversampling at the receiver [31].

C. Contributions

Focusing on Nyquist-rate sampling, and on the scenario where neither the transmitter nor the receiver have *a priori* CSI, we investigate the rates achievable over a frequency-flat Rayleigh block-fading massive MIMO channel, when the receiver is equipped with low-resolution ADCs. Our contributions are summarized as follows:

- Focusing on the one-bit ADC architecture, we generalize the analysis presented in [24] to include high-order modulations. We show that MRC/ZF detection combined with LS estimation at the BS allows for both multi-user operation and the use of high-order constellations such as 16-QAM, if the number of antennas is sufficiently large. Furthermore, the rates achievable with 16-QAM turn out to exceed the ones reported in [24] for QPSK, for SNR values as low as $-15\,\text{dB}$ per antenna, and for antenna arrays of 100 elements or more. Our results also suggest that there exists a trade-off between the number of BS antennas and the resolution of the ADCs used at each antenna port.
- Through a numerical study, we determine the minimum ADC resolution needed to make the performance gap to the infinite-precision case negligible. Our simulations suggest that only few bits (e.g., three to four) are required to achieve a performance close to the infinite-precision case for a large range of system parameters. For example, consider 10 users communicating with a BS that is equipped with 200 antennas. Furthermore, assume that the SNR is $-10\,\text{dB}$, that 64-QAM is selected, and that ZF is used at the BS. Then ADCs with three-bit resolution are sufficient to attain 97% of the infinite-precision per-user rate. This holds provided that all UEs are received with the same *average* power at the BS. In other words, when perfect power control is assumed.
- Finally, we assess the impact on performance of imperfect power control. Specifically, we characterize through numerical simulations the ADC resolution needed to separate the intended user from the interferers as a function of the signal-to-interference ratio (SIR). For example, when the number of antennas is 200 and the SIR is $-20\,\text{dB}$, the achievable per-user rate with three-bit ADCs is 89% of the infinite-precision rate. However, when the SIR is $-40\,\text{dB}$, three-bit ADCs achieve only 15% of the infinite-precision per-user rate. With one-bit ADCs, we attain only about 3% of the infinite-precision per-user rate at the same interference level.

This paper complements the analysis previously reported in [1] by generalizing it to ZF receivers, to multi-bit quantization, and to the case of imperfect power control. Furthermore, we develop an accurate and easy-to-evaluate high-SNR approximation to the rate achievable with QAM constellations and one-bit ADCs.

D. Notation

Lowercase and uppercase boldface letters denote column vectors and matrices, respectively. The identity matrix of size $N \times N$ is denoted by $\mathbf{I}_N$. We use $\mathrm{tr}\{\cdot\}$ to denote the trace of a matrix, and $\|\cdot\|$ to denote the ℓ_2-norm of a vector. The multivariate normal distribution with mean $\boldsymbol{\mu}$ and covariance Σ is denoted by $\mathcal{N}(\boldsymbol{\mu}, \Sigma)$. Furthermore, the multivariate complex-valued circularly-symmetric Gaussian probability density function with mean $\boldsymbol{\mu}$ and covariance Σ is denoted by $\mathcal{CN}(\boldsymbol{\mu}, \Sigma)$. The operator $\mathbb{E}_x[\cdot]$ stands for the expectation over the random variable x. The mutual information between two random variables x and y is indicated by $I(x; y)$. The real and imaginary parts of a complex scalar s are $\Re\{s\}$ and $\Im\{s\}$. The superscripts * and ^{H} denote complex conjugate and Hermitian transpose, respectively. The function $\Phi(x)$ is the cumulative distribution function (CDF) of a standard normal random variable.

E. Paper outline

The rest of the paper is organized as follows. In Section II, we introduce the massive MIMO system model. In Section III, we focus on the one-bit-ADC case and analyze the rate achievable with finite-cardinality constellations. We also derive a high-SNR approximation of the rate, which turns out to be accurate for a broad range of system parameters. In Section IV, we consider the case of multi-bit quantization and determine the ADC resolution required to approach the rate achievable in the infinite-precision case. We conclude in Section V.

II. System Model

We consider the single-cell uplink system depicted in Fig. 1. Here, K single-antenna users are served by a BS that is equipped with an array of $N \gg K$ antennas. We model the subchannels between each transmit-receive antenna pair as a Rayleigh block-fading channel (see, e.g., [32]), i.e., a channel that stays constant for T channel uses, and changes independently from block to block. We shall refer to T as the channel coherence interval. We further assume that the subchannels are mutually independent. The discrete-time complex baseband received signal over all antennas within an arbitrary coherence interval and before quantization is modeled as

$$\mathbf{y}_t = \mathbf{H}\mathbf{x}_t + \mathbf{w}_t, \quad t = 1, 2, \ldots, T. \tag{1}$$

Here, $\mathbf{x}_t \in \mathbb{C}^K$ denotes the channel input from all users at time t, and $\mathbf{H} \in \mathbb{C}^{N \times K}$ is the channel matrix connecting the K users to the N BS antennas. The entries of $\mathbf{H}$ are independent

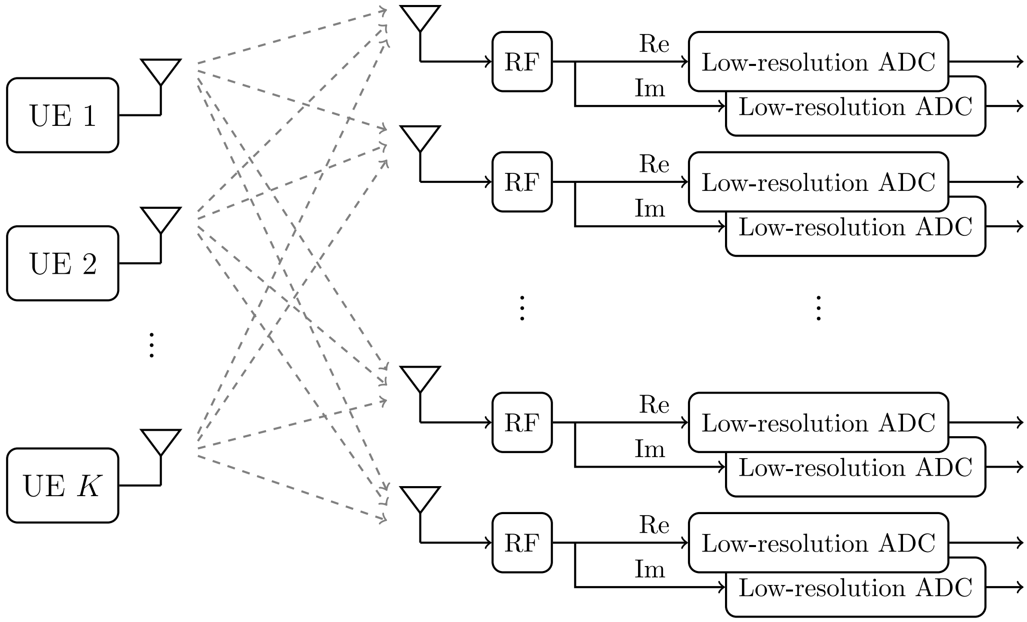

Fig. 1. Quantized massive MIMO uplink system model.

and $\mathcal{CN}(0, 1)$-distributed. Furthermore, the vector $\mathbf{w}_t \in \mathbb{C}^N$, whose entries are independent and $\mathcal{CN}(0, 1)$-distributed, stands for the AWGN.

The in-phase and quadrature components of the received signal at each antenna are quantized separately by an ADC of b-bit resolution. We characterize the ADC by a set of 2^b+1 quantization thresholds $\mathcal{T}_b = \{\tau_0, \tau_1, \ldots, \tau_{2^b}\}$, such that $-\infty = \tau_0 < \tau_1 < \cdots < \tau_{2^b} = \infty$, and a set of 2^b quantization labels $\mathcal{Q}_b = \{q_0, q_1, \ldots, q_{2^b-1}\}$ where $q_i \in (\tau_i, \tau_{i+1}]$. Let $\mathcal{R}_b = \mathcal{Q}_b \times \mathcal{Q}_b$. We shall describe the joint operation of the $2N$ b-bit ADCs at the BS by the function $Q_b(\cdot) : \mathbb{C}^N \to \mathcal{R}_b^N$ that maps the received signal $\mathbf{y}_t$ with entries $\{y_{n,t}\}$ into the quantized output $\mathbf{r}_t$ with entries $\{r_{n,t}\}$ in the following way: if $\Re\{y_{n,t}\} \in (\tau_k, \tau_{k+1}]$ and $\Im\{y_{n,t}\} \in (\tau_l, \tau_{l+1}]$, then $r_{n,t} = q_k + jq_l$. Using this convention, the quantized received signal can be written as

$$\mathbf{r}_t = Q_b(\mathbf{y}_t) = Q_b(\mathbf{H}\mathbf{x}_t + \mathbf{w}_t), \quad t = 1, 2, \ldots, T. \tag{2}$$

In the one-bit case, under the assumption that $\tau_1 = 0$ (zero-threshold comparator) and that $\mathcal{Q}_1 = \{-1, 1\}$, the quantization outcomes at each antenna belong to the set $\mathcal{R}_1 = \{1 + j, -1 + j, -1 - j, 1 - j\}$. Furthermore, we can write the quantized received signal at the nth antenna, at discrete time t, as follows:

$$r_{n,t} = Q_1(y_{n,t}) = \text{sgn}(\Re\{y_{n,t}\}) + j\text{sgn}(\Im\{y_{n,t}\}) \tag{3}$$

where $\mathrm{sgn}(\cdot)$ denotes the sign function defined as

$$\mathrm{sgn}(x) = \begin{cases} -1, & \text{if } x < 0 \\ 1, & \text{if } x \geq 0. \end{cases} \tag{4}$$

We consider the case where CSI is not available *a priori* to the transmitter or to the receiver, i.e., they are both not aware of the realization of $\mathbf{H}$. This scenario captures the cost of learning the fading channel [33]–[35], an operation that has to be performed using quantized observations. We further assume that coding can be performed over many coherence intervals. Let $\mathbf{X} = [\mathbf{x}_1, \mathbf{x}_2, \ldots, \mathbf{x}_T]$ be the $K \times T$ matrix of transmitted signals within a coherence interval, and let $\mathbf{R} = [\mathbf{r}_1, \mathbf{r}_2, \ldots, \mathbf{r}_T]$ be the corresponding $N \times T$ matrix of received quantized samples. For a given quantization function, the ergodic sum-rate capacity is [32]

$$C(\rho) = \frac{1}{T} \sup I(\mathbf{X}; \mathbf{R}). \tag{5}$$

Here, the supremum is over all probability distributions on $\mathbf{X}$ for which $\mathbf{X}$ has independent rows and the following average power constraint is satisfied:

$$\mathbb{E}\left[\mathrm{tr}\{\mathbf{X}\mathbf{X}^H\}\right] \leq KT\rho. \tag{6}$$

Since the noise variance is normalized to one, we can think of ρ as the SNR. The sum-rate capacity in (5) is, in general, not known in closed form, even in the infinite-precision case (for which tight capacity bounds have been reported recently in [36]).

A common approach to transmitting information over fading channels whose realizations are not known *a priori* to the receiver is to reserve a certain number of time slots in each coherence interval for the transmission of pilot symbols. These pilots are then used at the receiver to estimate the fading channel. Assume that P pilot symbols are used in each coherence interval ($K \leq P \leq T$). Because of the large dimensionality of the fading matrix $\mathbf{H}$, simple, low-complexity channel-estimation methods are favorable for massive MIMO [2]. Therefore, as in [24], we shall focus on LS channel estimation. For the one-bit SISO case, one can actually show that LS estimation combined with joint pilot and data processing (JPD) achieves the capacity [37], [1]. However, this result does not extend to MIMO systems. Although JPD processing is advantageous for low-resolution quantized massive MIMO [38], we will consider only the version of LS estimation that relies exclusively on pilot symbols and does not exploit JPD processing. Indeed, JPD processing is more computationally demanding and may not be suitable for massive MIMO.

We assume that the users are able to coordinate the transmission of their pilots: when one of the UEs transmits pilots, the other UEs remain idle. In other words, pilots are transmitted in a round robin fashion.[1] Furthermore, we assume that all users transmit the same number of pilots. According to the LS principle, an estimate of $\mathbf{H}$ is obtained as

$$\hat{\mathbf{H}} = \underset{\mathbf{H}}{\operatorname{argmin}} \sum_{t=1}^{P} \|\mathbf{r}_t - \mathbf{H}\mathbf{x}_t\|^2 \tag{7}$$

$$= \left(\sum_{t=1}^{P} \mathbf{r}_t \mathbf{x}_t^H\right) \left(\sum_{t=1}^{P} \mathbf{x}_t \mathbf{x}_t^H\right)^{-1}. \tag{8}$$

The use of time-interleaved pilots ensures that the matrix $\sum_{t=1}^{P} \mathbf{x}_t \mathbf{x}_t^H$ in (8) is indeed invertible. Also, because of the idle time, each user can transmit its pilots at a power level that is K times higher than the power level for the data symbols, while still satisfying the average-power constraint (6).

To limit the complexity further, we will focus on the case when the BS employs a linear receiver. Linear receiver processing—although inferior to nonlinear processing techniques such as successive interference cancellation—is less computationally demanding and has been shown to yield good performance if the number of antennas exceeds significantly the number of active users [39]. We shall consider two types of linear receivers, namely MRC and ZF. With MRC, we maximize the strength of a UEs signal, by using the channel estimates to combine the received signal coherently. In the infinite-precision case and if perfect CSI is available at the receiver, this results in an array gain proportional to N. With ZF, we additionally try to suppress the interference from other UEs at the cost of reducing the array gain to $N - K + 1$ (see, e.g., [39]). Using either of the two methods, a soft estimate $\hat{x}_{k,t}$ of the transmitted symbol $x_{k,t}$ from the kth user at time $t = P+1, P+2, \dots, T$ is obtained as follows:

$$\hat{x}_{k,t} = \mathbf{a}_k^H \mathbf{r}_t. \tag{9}$$

Here, $\mathbf{a}_k \in \mathbb{C}^N$ denotes the receive filter for the kth user, which is given by

$$\mathbf{a}_k = \begin{cases} \hat{\mathbf{h}}_k / \|\hat{\mathbf{h}}_k\|^2, & \text{for MRC} \\ (\hat{\mathbf{H}}^\dagger)_k, & \text{for ZF.} \end{cases} \tag{10}$$

With $\hat{\mathbf{h}}_k$ we denote the kth column of the matrix $\hat{\mathbf{H}}$, which is obtained through (8). Furthermore, $(\hat{\mathbf{H}}^\dagger)_k$ is the kth column of the pseudo-inverse of the channel estimate matrix $\hat{\mathbf{H}}^\dagger = \hat{\mathbf{H}}(\hat{\mathbf{H}}^H\hat{\mathbf{H}})^{-1}$.

[1]This pilot-transmission method is chosen for convenience; it may be suboptimal.

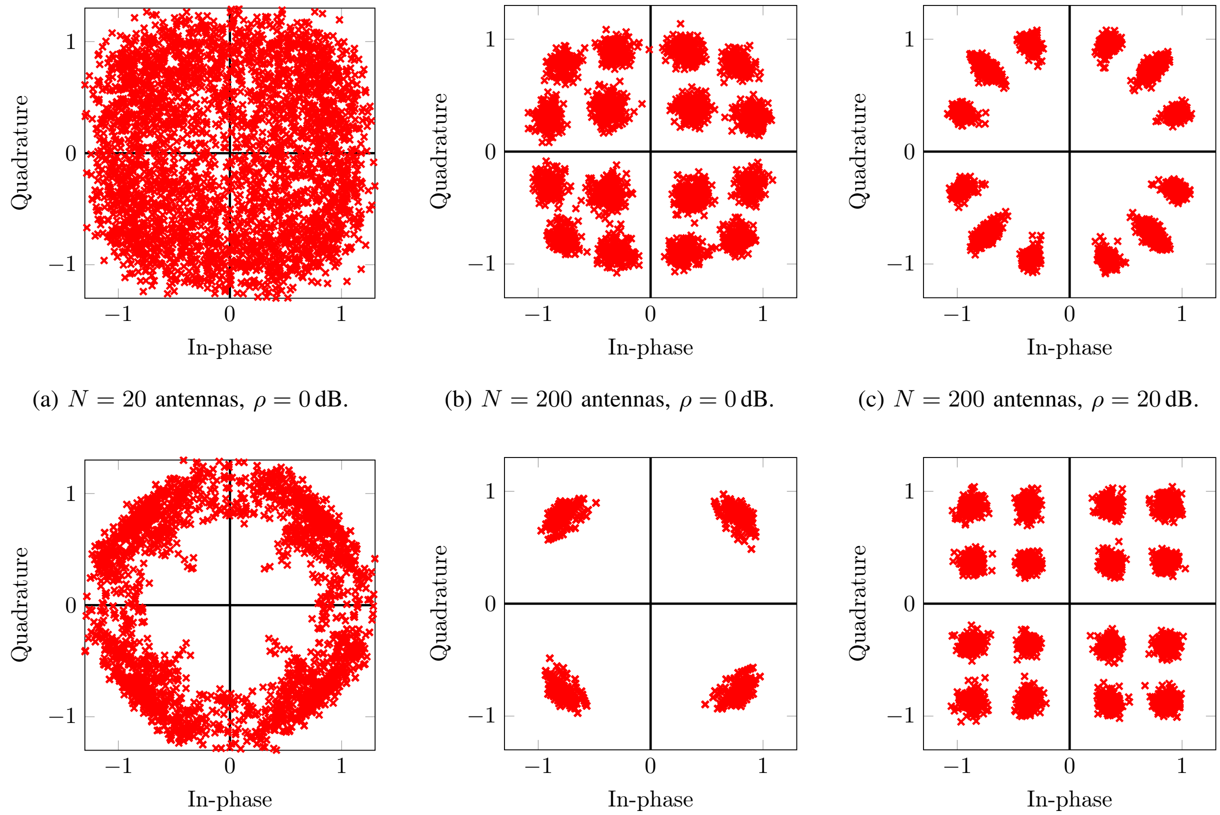

(a) $N = 20$ antennas, $\rho = 0\,\text{dB}$.

(b) $N = 200$ antennas, $\rho = 0\,\text{dB}$.

(c) $N = 200$ antennas, $\rho = 20\,\text{dB}$.

(d) $N = 200$ antennas, $\rho = 20\,\text{dB}$, correlated fading channel vector ($\mathbf{h} = h\mathbf{1}$).

(e) $N = 200$ antennas, $\rho = 20\,\text{dB}$, nonfading channel vector ($\mathbf{h} = \mathbf{1}$).

(f) $N = 200$ antennas, $\rho = 20\,\text{dB}$, nonfading channel vector ($\mathbf{h} = \mathbf{1}$), Gaussian dithering (11).

Fig. 2. Single-user MRC outputs for 16-QAM inputs as a function of the number of receive antennas N and the SNR ρ. The LS channel estimates are based on $P = 20$ pilot symbols.

III. Massive MIMO with One-Bit ADCs

In this section, we focus on the one-bit-ADC case and assess the rates achievable with QAM constellations of varying size.

A. *High-order Modulation Formats with One-bit ADCs: Why Does it Work?*

1) The role of additive noise: Although QPSK is optimal in the SISO case, the use of multiple antennas at the receiver opens up the possibility of using higher-order modulation schemes to support higher rates. This observation is demonstrated in Fig. 2 where we plot the MRC receiver output (for 300 different channel fading realizations) corresponding to 16-QAM data symbols for the case when a single user transmits also $P = 20$ pilots to let the BS acquire LS channel estimates. As the size of the BS antenna array increases, the 16-QAM constellation becomes progressively distinguishable (see Fig. 2b), provided that ρ is not too high. Indeed, additive noise is one of the factors that enables the detection of the 16-QAM constellation; the other is the different phase of the fading coefficients associated with each receive antenna. The explanation is as follows: due to the one-bit ADCs, the quantized received output at each antenna belongs to the set $\mathcal{R}_1$ of cardinality 4. These 4 possible outputs are then averaged by the MRC filter to produce an output (a scalar) that belongs to an alphabet with much higher cardinality. The cardinality depends on the number of pilots and on the number of receive antennas. The key observation is that the inner points of the 16-QAM constellation, which are more susceptible to noise, are more likely to be erroneously detected at each antenna. This results in a smaller averaged value after MRC than for the outer constellation points. To highlight the importance of the additive noise, we consider in Fig. 2c the case when $\rho = 20\,\mathrm{dB}$. Since the additive noise is negligible, the output of the MRC filter lies approximately on a circle, which suggests that the amplitude of the transmitted signal cannot be used to convey information. However, the phase of the 16-QAM symbols can still be detected. Indeed, because of the independent fading, the phase distortion caused by the coarse quantization, which is significant at each antenna, is zero-mean and will therefore be averaged out with MRC.

2) Impact of spatial correlation: If the fading coefficients are correlated over the antenna array, the ability to recover the phase of the transmitted signal may be lost at high SNR. To demonstrate this, let $\mathbf{h} = h\mathbf{1}$ with $h \sim \mathcal{CN}(0, 1)$, denote the channel fading vector. Here, $\mathbf{1}$ is the all-one vector. For this case, the phase distortion due to fading is equal on all antennas and it can no longer be averaged out with MRC (see Fig. 2d). When the noise is negligible and when the channel is nonfading (i.e., when $\mathbf{h} = \mathbf{1}$) the constellation collapses to a noisy QPSK diagram (see Fig. 2e). For both of these unfavorable cases, high-order modulations are not supported by the channel.

3) Dithering: A possible remedy to this problem is to randomize the quantization error among observations by intentionally adding noise to the signal prior to the ADC. This approach is commonly referred to as *dithering*, and its advantages are well documented (see, e.g., [40]–[42]). We can write the quantized dithered signal at time t as

$$\mathbf{r}_t = Q_1(\mathbf{h}x_t + \mathbf{w}_t + \mathbf{d}_t), \quad t = 1, 2, \ldots, T \tag{11}$$

where $\mathbf{d}_t \in \mathbb{C}^N$ is the dither signal at time t.

To highlight the benefits of dithering, we consider again the case when $\mathbf{h} = \mathbf{1}$ and $\rho = 20\,\mathrm{dB}$, and show in Fig. 2f the received 16-QAM constellation after we have applied dithering. Similarly to [26], we have used a $\mathcal{CN}(\mathbf{0}, (\rho-1)\mathbf{I}_N)$-distributed dither signal. We note that it is now possible to detect the 16-QAM symbols. Dithering can also be used to recover the 16-QAM constellations in Fig. 2c and 2d, for the independent and correlated Rayleigh-fading case, respectively.

Dithering (which requires knowledge about the SNR) can be implemented by, for example, adding DC biases to the comparators in the ADCs. Since we strive to keep the receiver hardware complexity at a minimum, we will only consider nondithered quantization in the remainder of this paper. For the independent Rayleigh-fading case considered in this paper, dithering is useful at high SNR. However, in massive MIMO, the SNR per antenna is typically low, as we rely on the massive number of antennas to provide large array gain. Furthermore, in a multi-user scenario, the interference from other UEs will also perturb the signal, causing beneficial randomization in the quantization error.

B. Sum-rate Capacity Lower-Bound

It follows from, e.g., [43], that the achievable rate $R^{(k)}(\rho)$ for user $k = 1, 2, \ldots, K$ with LS estimation and MRC or ZF detection is

$$R^{(k)}(\rho) = \frac{T-P}{T} I(x_k; \hat{x}_k \,|\, \hat{\mathbf{H}}) \tag{12}$$

where x_k and $\hat{x}_k$ are distributed as $x_{k,t}$ and $\hat{x}_{k,t}$ respectively. It follows that the sum-rate capacity can be lower-bounded as follows:

$$C(\rho) \geq \sum_{k=1}^{K} R^{(k)}(\rho). \tag{13}$$

In order to compute the achievable rate, we expand the mutual information in (12) as follows

$$I(x_k; \hat{x}_k \,|\, \hat{\mathbf{H}}) = \mathbb{E}_{x_k, \hat{x}_k, \hat{\mathbf{H}}}\left[\log_2 \frac{P_{\hat{x}_k|x_k,\hat{\mathbf{H}}}(\hat{x}_k|x_k,\hat{\mathbf{H}})}{P_{\hat{x}_k|\hat{\mathbf{H}}}(\hat{x}_k|\hat{\mathbf{H}})}\right]. \tag{14}$$

Computing (14) requires one to obtain the conditional probability mass functions $P_{\hat{x}_k|x_k,\hat{\mathbf{H}}}(\hat{x}_k|x_k,\hat{\mathbf{H}})$ and $P_{\hat{x}_k|\hat{\mathbf{H}}}(\hat{x}_k|\hat{\mathbf{H}}) = \mathbb{E}_{x_k}\left[P_{\hat{x}_k|x_k,\hat{\mathbf{H}}}(\hat{x}_k|x_k,\hat{\mathbf{H}})\right]$. Since no closed-form expressions are available, one needs to estimate them by Monte-Carlo sampling, i.e., by simulating many noise and interference realizations, and by mapping the resulting $\hat{x}_k$ to points over a rectangular grid in the complex plane as described in [24]. With this technique, we obtain a lower bound on $R^{(k)}(\rho)$ [44, p. 3503] that becomes increasingly tight as the grid spacing is made smaller.[2] Note that (14) holds for every choice of input distribution and for ADCs with arbitrary resolution. In the remainder of this section, we will however focus on one-bit ADCs and QAM constellations.

C. High-SNR Approximation of the Achievable Rate

Evaluating the conditional probabilities in (14) is tedious as it involves the simulation of a large number of noise and interference trials for each realization of the channel $\mathbf{H}$. We next provide an accurate high-SNR approximation of (12) that is easier to compute in practice. Our high-SNR approximation relies on the following assumptions:

- a single pilot per user suffices to accurately estimate the sign of the real and imaginary part of each entry of the channel matrix;
- the real part $\hat{x}_k^R = \Re\{\hat{x}_k\}$ and the imaginary part $\hat{x}_k^I = \Im\{\hat{x}_k\}$ of the soft estimate $\hat{x}_k$ of the transmitted symbol x_k are conditionally jointly Gaussian given x_k and $\hat{\mathbf{H}}$, with conditional mean $\boldsymbol{\mu}(x_k, \hat{\mathbf{H}})$ and conditional covariance $\Sigma(x_k, \hat{\mathbf{H}})$.

These assumptions result in

$$R^{(k)}(\rho) \approx \frac{T-K}{T}\left(h\Big(\hat{x}_k^R,\, \hat{x}_k^I \,|\, \hat{\mathbf{H}}\Big) - \frac{1}{2}\,\mathbb{E}_{x_k,\hat{\mathbf{H}}}\Big[\log_2\Big((2\pi e)^2 \det \Sigma(x_k, \hat{\mathbf{H}})\Big)\Big]\right). \tag{15}$$

Here, $h(\cdot)$ denotes the differential entropy of a random vector [45]. In Appendix A, we provide closed-form expressions for the mean $\boldsymbol{\mu}(x_k, \hat{\mathbf{H}})$ and the variance $\Sigma(x_k, \hat{\mathbf{H}})$ for the MRC case (see (29)–(33)). For the ZF case, the mean is provided in (34) whereas we resort to Monte-Carlo simulations to compute its covariance matrix. As we will illustrate in Section III-D, the approximation (15) turns out to be accurate over a large range of SNR values.

D. Numerical Evaluation of the Achievable Rate

We now assess the rates achievable with LS estimation on a multi-user massive MIMO uplink channel when the receiver is equipped with one-bit ADCs.

[2] The numerical routines used to evaluate (12) can be downloaded at https://github.com/infotheorychalmers/one-bit_massive_MIMO.

1) Single-user case: In Fig. 3 we compare for the single-user case, the rates achievable with QPSK, 16-QAM, and 64-QAM as a function of ρ.[3] We depict both the rates achievable with one-bit ADCs and the ones for the infinite-precision case. The rates with one-bit ADCs, which are computed using (12) and (14), are compared with the approximation provided in (15) to verify its accuracy. The infinite-precision rates are computed using (12) and (14); indeed the evaluation of these expression can be effected efficiently in the infinite precision case. The number of receive antennas is $N = 200$, and the coherence interval is $T = 1142$.[4] The number of transmitted pilots P is numerically optimized for every value of ρ. We see that, despite using one-bit ADCs, higher-order modulations outperform QPSK already at SNR values as low as $\rho = -15\,\text{dB}$. Note that the achievable rate does not increase monotonically with ρ in the 16-QAM and 64-QAM case. Indeed, as ρ gets large the constellation gets projected onto the unit circle and the number of distinguishable constellation points becomes smaller (see Fig. 2c). Note also that the high-SNR approximation (15) closely tracks the simulation results for SNR values as low as $-10\,\text{dB}$.[5] The proposed approximation (15) enables us to accurately predict the SNR value beyond which the rates achievable with a given constellation saturates. This, in turn, allows us to identify the most appropriate constellation for a given SNR value.

We note that, when QPSK is used, the difference in the achievable rates between the one-bit quantized case and the infinite-precision case is marginal—an observation that was already reported in [24]. In contrast, the rate loss is more pronounced for higher-order constellations.

2) Multi-user case: In Fig. 4, we plot the rates achievable with MRC and ZF for both the one-bit-ADC and the infinite-precision case when $K = 10$ users are active.[6] Motivated by the results in Fig. 3, we only compare the rates achievable with 16-QAM and 64-QAM. Note again that the high-SNR approximation (15) turns out to be accurate for a large range of SNR values.

[3]To evaluate the mutual information (14), we have simulated 300 random fading channel realizations. For each channel realization we have considered 3000 random noise realizations for each symbol in the transmitted constellation.

[4]For an LTE-like system operating at 2 GHz, with symbol time equal to $66.7\,\mu\text{s}$, and with UEs moving at a speed of $3\,\text{km/h}$, the duration of the coherence interval according to Jake's model is approximately $T = 1142$ symbols.

[5]The accuracy of the approximation (15) at low SNR values depends critically on T; the approximation tends to overestimate the rate for low values of T and to underestimate the rate for large value of T.

[6]To evaluate the mutual information (14), we have simulated 300 random fading channel realizations. For each channel realization we have considered 3000 random noise and interference realizations for each user and each symbol in the transmitted constellation.

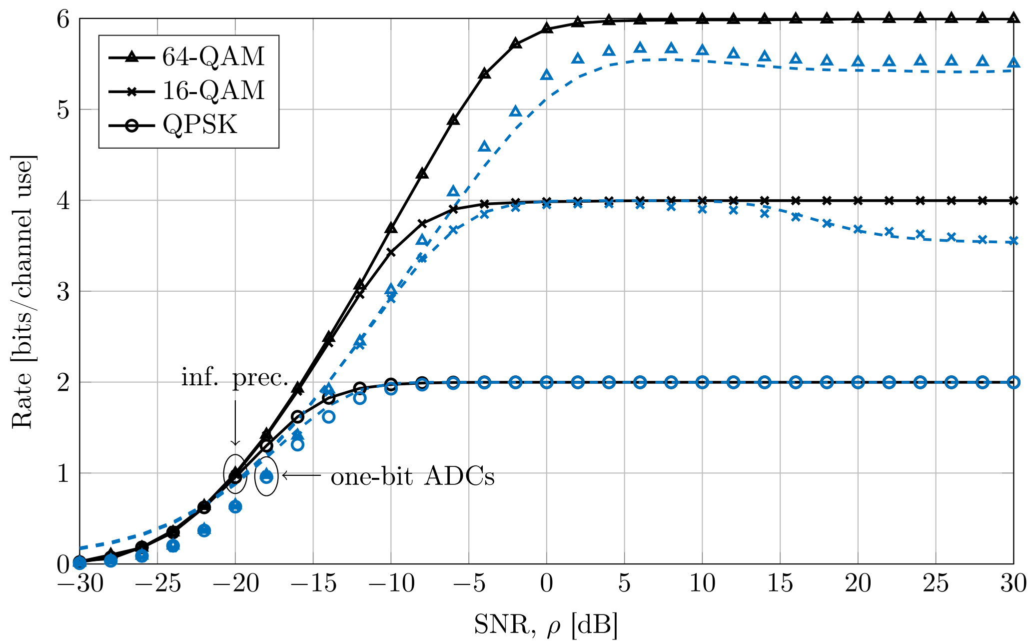

Fig. 3. Single-user achievable rate with LS estimation and MRC as a function of the SNR ρ; $N = 200$, $K = 1$, $T = 1142$; the number of pilots P is optimized for each value of ρ. The dashed lines correspond to the high-SNR approximation (15), and the marks correspond to the rates computed via (12) and (14).

For the one-bit-ADC case, independently of whether MRC or ZF is used, the rate per user is significantly reduced compared to the single-user case (cf. Fig. 3). This suggests that, with high-order modulations, the system becomes interference limited because the one-bit ADCs partially destroy the orthogonality between the fading channels associated with different users. In fact, there is virtually no difference between the single-user and the multi-user rate in the infinite-precision case if ZF is used (cf. Fig. 3 and Fig. 4b). In contrast, when MRC is employed, the system is interference limited also in the infinite-precision case.

More pilots are required in the one-bit-ADC case compared to the infinite-precision case, as it is more challenging to perform channel estimation based on the coarsely quantized observations. For example, when $\rho = 10\,\text{dB}$, and one uses 16-QAM in combination with ZF, the optimal number of pilots in the infinite-precision case is one per user, whereas in the one-bit-ADC case it is five per user.

3) Dependence on the number of BS antennas: In Fig. 5, we plot the per-user achievable rates as a function of the number of BS antennas. Here, $\rho = -10\,\text{dB}$, $K = 10$, and $T = 1142$. As in the previous cases, the number of pilot symbols is optimized, this time for each value of N.

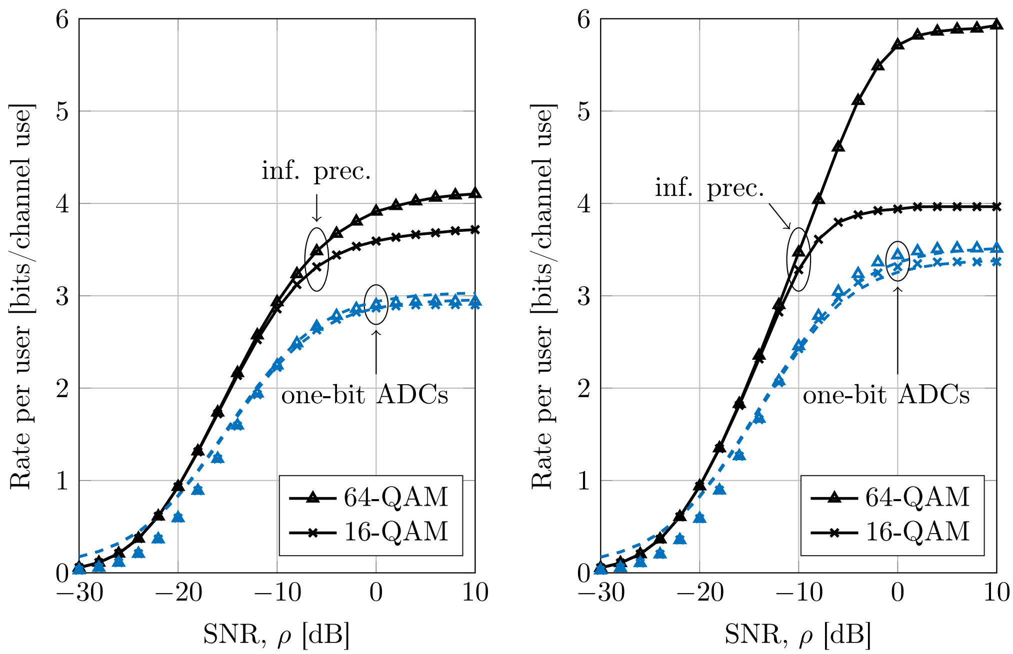

(a) MRC receiver.

(b) ZF receiver.

Fig. 4. Per-user achievable rate with LS estimation as a function of the SNR ρ; $N = 200$, $K = 10$, $T = 1142$; the number of pilots P is optimized for each value of ρ. The dashed lines correspond to the high-SNR approximation (15), and the marks correspond to the rates computed via (12) and (14).

The high-SNR approximation is again shown to be accurate for all values of N, despite the low value of ρ. We note that higher-order constellations outperform QPSK also when the number of receive antennas is much smaller than 200. Furthermore, when QPSK is used, the achievable rate saturates rapidly as the number of receive antennas is increased.

4) Dependence on the coherence interval: In Fig. 6, we plot the per-user achievable rates with ZF, as a function of the coherence interval T for $\rho = -10\,\text{dB}$, $N = 200$, and $K = 10$. Here, the rates are computed via (12) and (14). The number of pilot symbols is numerically optimized for each value of T. We also depict the achievable rates for the perfect-CSI case. Similarly to the SISO case (see [1]), as T increases the per-user achievable rate approaches the perfect receiver-CSI rate. However, this convergence occurs at a slower pace than for the infinite-precision case. This suggests that the one-bit ADC architecture is less suitable for high-mobility scenarios. Note also that the achievable rate is zero when $T \leq 10$. In fact, when orthogonal pilot sequences are transmitted, at least 10 pilot symbols are required when $K = 10$.

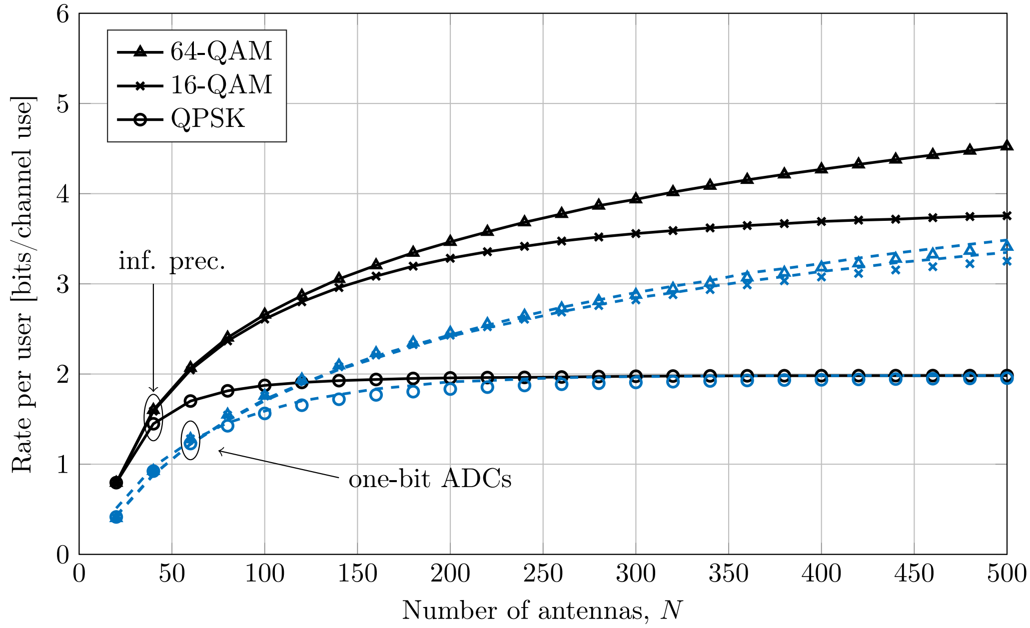

Fig. 5. Per-user achievable rate with LS estimation and ZF as a function of N; $\rho = -10\,\text{dB}$, $K = 10$, $T = 1142$; the number of pilots P is optimized for each value of N. The dashed lines correspond to the high-SNR approximation (15), and the marks correspond to the rates computed via (12) and (14).

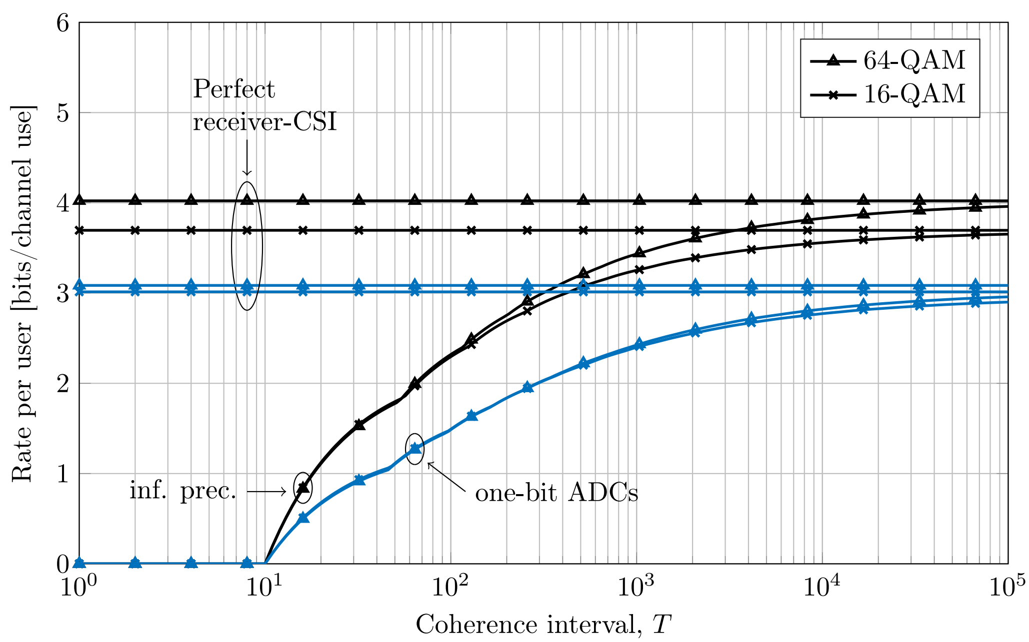

Fig. 6. Per-user achievable rate with LS estimation and ZF as a function of T; $\rho = -10\,\text{dB}$, $N = 200$, $K = 10$; the number of pilots P is optimized for each value of T.

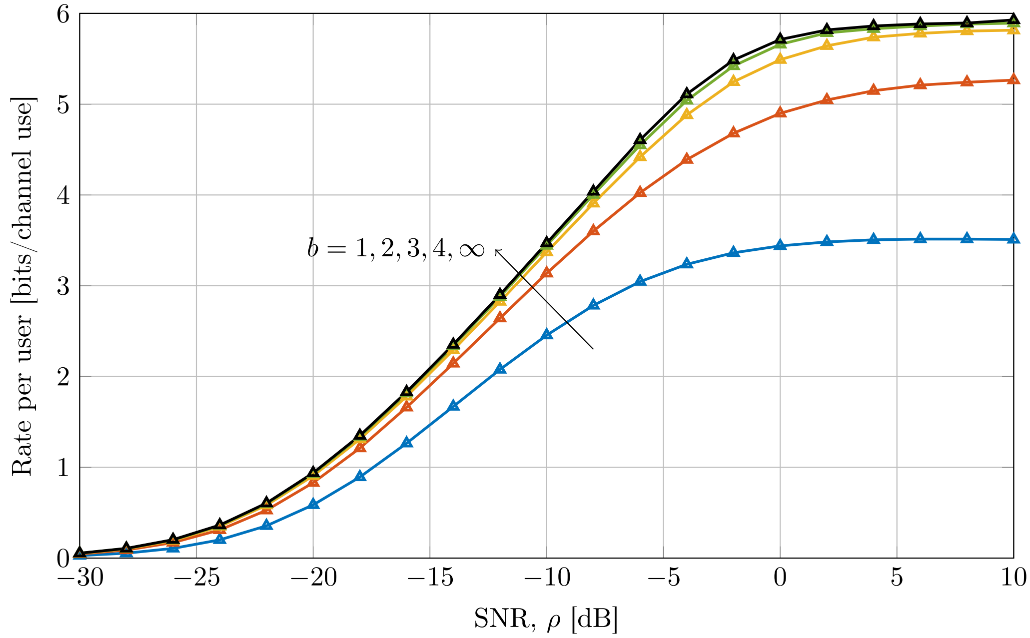

Fig. 7. Per-user achievable rate with LS estimation, 64-QAM, and ZF as a function of the SNR ρ; $N = 200$, $K = 10$, $T = 1142$; the number of pilots P is optimized for each value of ρ.

IV. Massive MIMO with Multi-Bit ADCs

We now turn our attention to the multi-bit-ADC case. To determine the quantization labels and levels we approximate the channel output by a Gaussian random variable and use the Lloyd-Max algorithm [46], [47].[7] The motivation behind the Gaussian approximation is that the per-antenna received signal converges to a Gaussian random variable with zero mean and variance $K\rho + 1$ as the number of users grows.

A. Dependence on ADC resolution

Focusing on 64-QAM and ZF, we compare in Fig. 7 the achievable rate computed using (12) and (14) as a function of the ADC resolution and the SNR.[8] We observe that with two-bit ADCs, the achievable rate increases significantly compared to the one-bit-ADC case. For example, at $\rho = -10\,\text{dB}$, we achieve 90% of the infinite-precision rate, compared to 71% with one-bit ADCs.

[7]For the system-parameter values chosen in this section, a uniform quantizer yields similar performance.

[8]Also in the multi-bit-ADC case, one can derive a Gaussian approximation to the achievable rate similar to (15), this approximation is not detailed for space constraints.

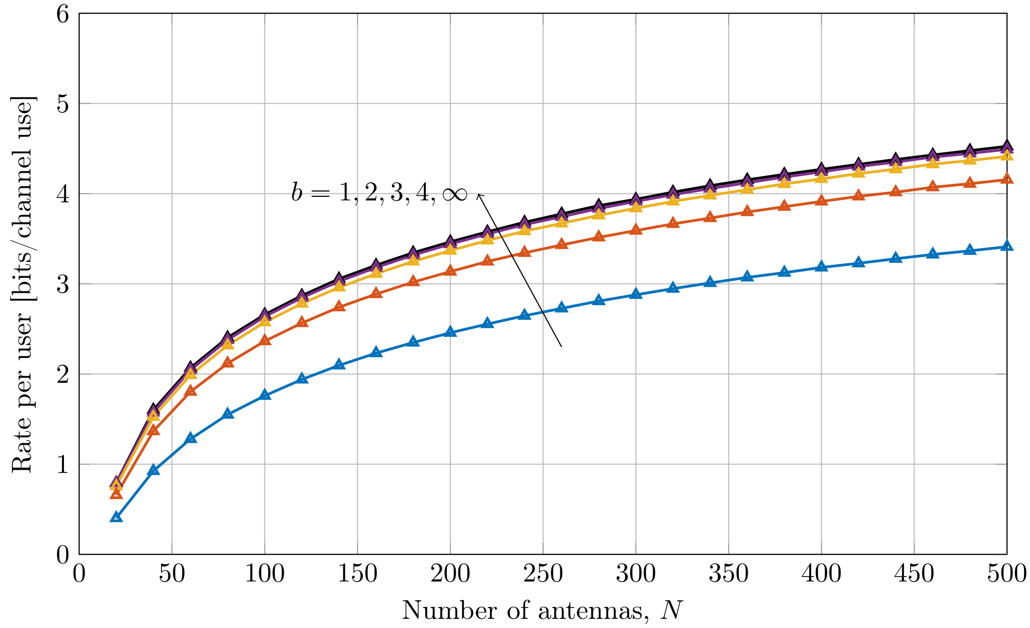

Fig. 8. Per-user achievable rate with LS estimation, 64-QAM, and ZF as a function of the N; $\rho = -10\,\text{dB}$, $K = 10$, $T = 1142$; the number of pilots P is optimized for each value of ρ.

Increasing the ADC resolution beyond four bits seems unnecessary for the system parameters considered in Fig. 7.

In Fig. 8, we compare the achievable rate as a function of the ADC resolution and the number of BS antennas. We observe that the use of ADCs with only three-bit resolution entails virtually no loss in terms of achievable rate compared to the infinite-precision case, for the entire range of N shown in the figure. Furthermore, to achieve 3 bits per channel use in the one-bit-ADC case, about 360 antennas are required. In contrast, for the two-bit-ADC case only 180 antennas are required to meet the same target rate, and for the three-bit-ADC case, 160 antennas suffice. We thus observe that there exists a trade-off between the number of BS antennas and the resolution of the ADCs required at each antenna port. We note that when deciding on whether to equip a BS with a large number of antennas and low-resolution ADCs, or to equip it with fewer antennas but with high-precision ADCs, the power consumption of the ADCs along with that of other hardware components in the transceivers has to be taken into account.

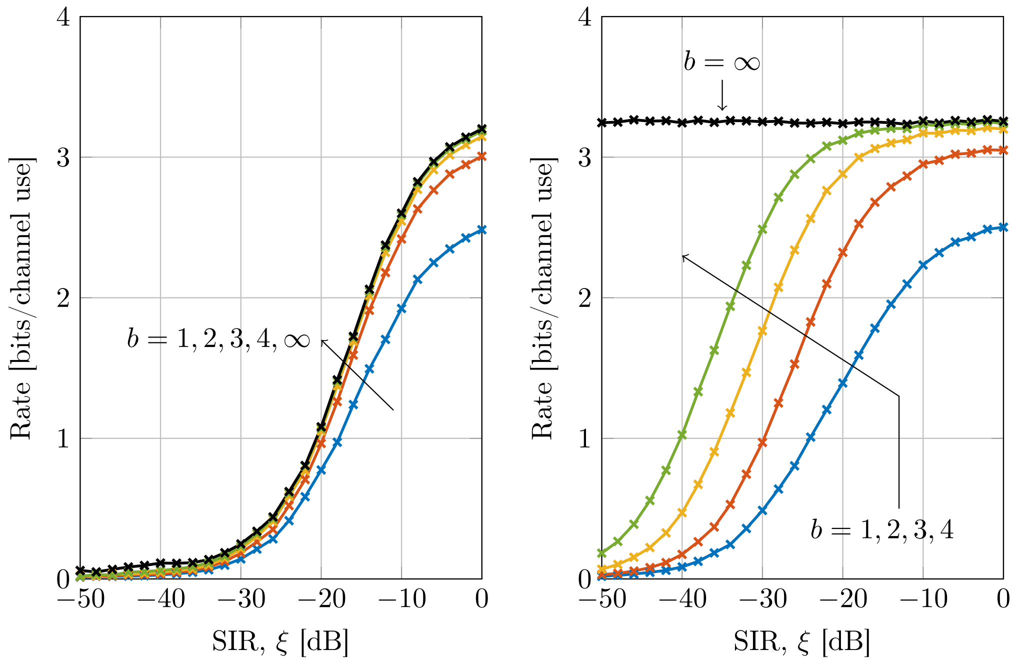

(a) MRC receiver.

(b) ZF receiver.

Fig. 9. Achievable rate with LS estimation and 16-QAM as a function of the SIR ξ; $\rho_1 = -10\,\text{dB}$, $N = 200$, $K = 10$, $T = 1142$, and $P = 10$.

B. Impact of Large-Scale Fading and Imperfect Power Control

So far, we have considered only the case when all users operate at the same average SNR. This corresponds to the scenario where perfect power control can be performed in the uplink, which is clearly favorable for low-resolution ADC architectures. If, however, the received signal powers are vastly different, low-power signals may not be distinguishable from high-power interferers for cases in which the ADCs resolution is too low. To investigate this issue, we consider first the case when there are only two users in the cell. Both users transmit 16-QAM symbols, the first one with SNR $\rho_1 = -10\,\text{dB}$, the second one with a varying transmit power. Specifically, its SNR ρ_2 ranges from $-10\,\text{dB}$ to $50\,\text{dB}$. Hence, the SIR for the first user before receiver filtering is $\xi = \rho_1/\rho_2$ (in linear scale).

In Fig. 9, we plot the achievable rates for the first user, for varying ADC resolution, as a function of the SIR. As before, $N = 200$ and $T = 1142$. We set the number of pilots per user to $P/K = 10$. Note that the interfering signal is in-band and can not be removed by RF filtering. With MRC, the system is sensitive to interference even in the infinite-precision case. Consequently, increasing the ADC resolution beyond three bits provides no gain in terms of

TABLE I

SUMMARY OF SIMULATION PARAMETERS

Description	Assumption
Cell layout	Circular cell
Cell radius	335 meters
Minimum distance between UE and BS	35 meters
Path loss	$35 + 35 \log_{10}(d)$ dB
Number of BS antennas (N)	200 antennas
Number of single-antenna users (K)	10 users
Coherence interval (T)	1142 channel uses
Number of pilots per user (P/K)	10 pilots per user
Carrier frequency	2 GHz
System bandwidth	20 MHz
UE transmit power	8.5 dBm
Noise spectral efficiency	-174.2 dBm/Hz
Noise figure	5 dB

interference mitigation. In contrast, with ZF the system can handle substantially more interference. Indeed, in the infinite-precision case, the achievable rate is unaffected by the interference. With one-bit ADCs on the other hand, the interference cannot be mitigated. For example, at SIR $\xi = -20$ dB the rate drops to 43% of the infinite-precision case. For SIR $\xi = -40$ dB, less than 3% is attained. By increasing the resolution beyond one bit, the system can tolerate more interference. For three-bit ADCs, we achieve 89% and 15% of the infinite-precision rate when the SIR is -20 dB and -40 dB, respectively.

In practical systems, large spreads in the received power is typically avoided through power control. However, perfect power control may be impossible to achieve in practice due to limitations on the UE transmit power, for example. We next investigate how relaxing the accuracy of the UE transmit power control will impact the system performance. We consider a single-cell scenario and adapt the urban-macro path loss model in [48]. The simulation parameters for this study are summarized in Table I. The transmit power for all UEs is set to 8.5 dBm, which for the first user that is located $d_1 = 185$ meters from the BS, results in a SNR of approximately $\rho_1 = -10$ dB. The remaining $K - 1$ users in the cell are randomly dropped according to a uniform distribution on the circular ring of inner radius $d_1 - \Delta d$ meters and outer radius $d_1 + \Delta d$ meters, for a

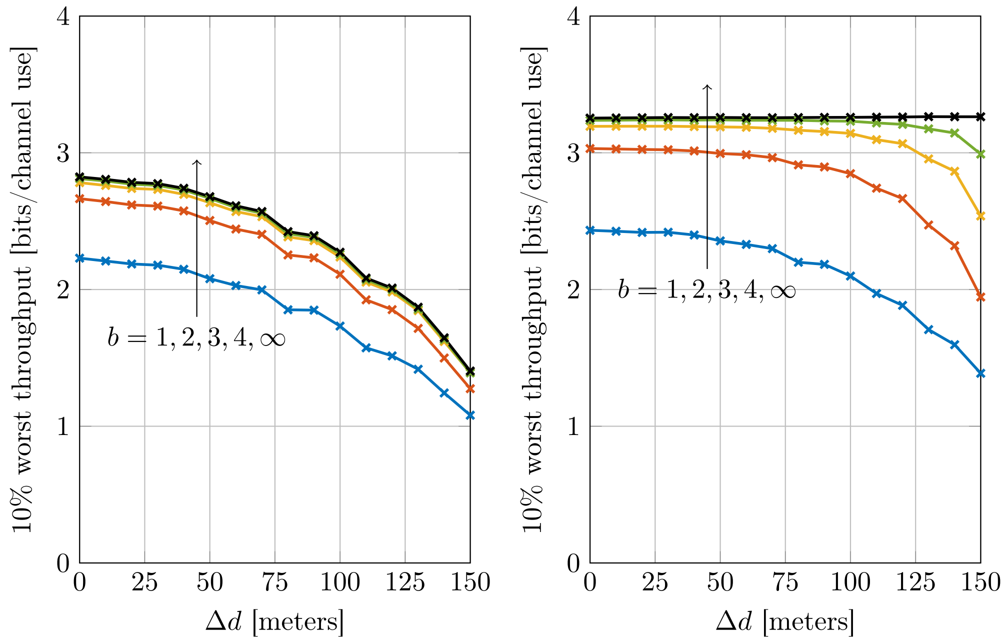

(a) MRC receiver. (b) ZF receiver.

Fig. 10. The 10% worst throughput with LS estimation and 16-QAM for a user located $d_1 = 185$ meters away from the BS as a function of Δd for the parameters specified in Table I.

distance spread $0 < \Delta d < 150$ meters. The case $\Delta d = 0$ corresponds to the scenario when power control is executed perfectly. The case $\Delta d = 150$ meters corresponds to the worst-case scenario of *uncoordinated* uplink transmission, where no power control is performed by the UEs. In the latter case, the SNR for each interfering user lies in the range $[-19.0\,\text{dB},\ 15.3\,\text{dB}]$.

In Fig. 10, we plot the 10% worst throughput (i.e., the throughput corresponding to the 10% point of the CDF of throughputs), for the intended user located $d_1 = 185$ meters away from the BS, as a function of Δd. We focus on 16-QAM and assume that the received signal power level for each user is known to the BS. To attain the curves, we have considered 1000 random interfering user drops for each Δd value.[9] As expected, the gap to the infinite-precision rate grows as Δd increases. In the uncoordinated case, with one-bit ADCs and ZF, we attain 57% of the rate achievable with perfect power control. The corresponding number for the three-bit-ADC case is 79%. This shows that high rates are achievable with low-resolution ADCs even in absence of power control.

[9] To compute the rate in (12), we simulate 300 random fading channel realizations for each user drop.

V. Conclusions

We have analyzed the performance of a low-resolution quantized uplink massive MIMO system operating over a frequency flat Rayleigh block-fading channel whose realizations are not known *a priori* to transmitter and receiver.

We have shown that for the one-bit massive MIMO case, high-order constellations, such as 16-QAM, can be used to convey information at higher rates than with QPSK. This holds in spite of the nonlinearity introduced by the one-bit quantizers. Furthermore, reliable communication can be achieved by using simple signal processing techniques at the receiver, i.e., LS channel estimation and MRC detection.

By increasing the resolution of the ADCs by only a few bits, e.g., to three or four bits, we can achieve near infinite-precision performance for a large range of system parameters. Furthermore, the system becomes robust against differences in the received signal power from the different users, due for example, to large-scale fading or imperfect power control.

An extension of our analysis to a OFDM based setup for transmission over frequency-selective channels is currently under investigation. Such an extension could be used to benchmark the results recently reported in [28] in which the authors reported that, with a specific modulation and coding scheme taken from IEEE 802.11n, four to six bits are required to achieve a packet error rate below 10^{-2} at an SNR close to the one needed in the infinite-precision case. We conclude that for a fair comparison between the performance attainable using low-resolution versus high-resolution ADCs, one should take into account the overall power consumption, including the power consumed by RF and baseband processing circuitry.

Appendix A
Derivation of (15)

To attain the high-SNR approximation (15), we shall assume that a single pilot per user is sufficient to correctly estimate the quadrant in which each entry of the channel matrix $\mathbf{H}$ lies. In this case, the channel estimate in (8) reduces to

$$\hat{\mathbf{H}} = \operatorname{sgn}\{\Re\{\mathbf{H}\}\} + j\operatorname{sgn}\{\Im\{\mathbf{H}\}\}. \tag{16}$$

In what follows, we will derive a closed-form approximation to the achievable rate (12) under the assumption that the estimate in (16) is known to the receiver. To this end, we first need to determine the real and imaginary parts of the received signal. To keep the notation compact, we set

$\hat{x}_k^R = \Re\{\hat{x}_k\}$ and $\hat{x}_k^I = \Im\{\hat{x}_k\}$. Furthermore, by writing $a_{n,k} = a_{n,k}^R + ja_{n,k}^I$, $h_{n,k} = h_{n,k}^R + jh_{n,k}^I$, and $r_n = r_n^R + jr_n^I$, where $a_{n,k}$ denotes the nth entry of the receive filter $\mathbf{a}_k$ and r_n the nth entry of the received vector $\mathbf{r}$, we can express the real components of the received signal as

$$\hat{x}_k^R = \sum_{n=1}^{N} \Re\{a_{n,k}^* r_n\} = \sum_{n=1}^{N} \left(a_{n,k}^R r_n^R + a_{n,k}^I\, r_n^I\right) = \sum_{n=1}^{N} \left(\frac{a_{n,k}^R}{\operatorname{sgn}\{h_{n,k}^R\}} c_n^{R,R} + \frac{a_{n,k}^I}{\operatorname{sgn}\{h_{n,k}^I\}}\, c_n^{I,I} \right). \quad (17)$$

Here, we have defined $c_n^{R,R} = \operatorname{sgn}\{h_{n,k}^R\} r_n^R$ and $c_n^{I,I} = \operatorname{sgn}\{h_{n,k}^I\} r_n^I$. Similarly, for the imaginary part we can write

$$\hat{x}_k^I = \sum_{n=1}^{N} \Im\{a_{n,k}^* r_n\} = \sum_{n=1}^{N} \left(a_{n,k}^R r_n^I - a_{n,k}^I\, r_n^R\right) = \sum_{n=1}^{N} \left(\frac{a_{n,k}^R}{\operatorname{sgn}\{h_{n,k}^R\}} c_n^{R,I} - \frac{a_{n,k}^I}{\operatorname{sgn}\{h_{n,k}^I\}}\, c_n^{I,R} \right). \quad (18)$$

Here, we have defined $c_n^{R,I} = \operatorname{sgn}\{h_{n,k}^R\} r_n^I$ and $c_n^{I,R} = \operatorname{sgn}\{h_{n,k}^I\} r_n^R$.

Now, we collect the real and imaginary components in a vector $[\hat{x}_k^R,\, \hat{x}_k^I]^T$ and approximate their conditional distribution given the channel input and the channel estimate as a bivariate Gaussian random vector with mean $\boldsymbol{\mu}(x_k, \hat{\mathbf{H}})$ and 2×2 covariance matrix $\Sigma(x_k, \hat{\mathbf{H}})$. It follows that the mutual information in (14) can be approximated as

$$I(x_k; \hat{x}_k \,|\, \hat{\mathbf{H}}) \approx h\Big(\hat{x}_k^R,\, \hat{x}_k^I \,|\, \hat{\mathbf{H}}\Big) - \frac{1}{2}\, \mathbb{E}_{x_k, \hat{\mathbf{H}}} \Big[\log_2 \Big((2\pi e)^2 \det \Sigma(x_k, \hat{\mathbf{H}}) \Big)\Big]. \quad (19)$$

Here, the differential entropy $h(\hat{x}_k^R,\, \hat{x}_k^I \,|\, \hat{\mathbf{H}})$ is evaluated by assuming that $[\hat{x}_k^R,\, \hat{x}_k^I]^T$ is conditionally Gaussian given x_k and $\hat{\mathbf{H}}$, which implies that for inputs drawn from a QAM constellation, the conditional probability of $[\hat{x}_k^R,\, \hat{x}_k^I]^T$ given $\hat{\mathbf{H}}$ is a Gaussian mixture. The achievable rate in (15) follows from (19) by taking into account the rate loss due to the transmission of $P = K$ pilot symbols (one per user) to estimate the channel. We shall next discuss how to choose $\boldsymbol{\mu}(x_k, \hat{\mathbf{H}})$ and $\Sigma(x_k, \hat{\mathbf{H}})$.

We start by finding a suitable approximation for the probability mass functions of the binary random variables $c_n^{R,R}$, $c_n^{I,I}$, $c_n^{R,I}$ and $c_n^{I,R}$, whose support is $\{-1, +1\}$. For $c_n^{R,R}$, it holds that

$$\begin{aligned} \Pr\left\{c_n^{R,R} = 1\right\} &= \Pr\left\{\operatorname{sgn}\{h_{n,k}^R\} r_n^R = 1\right\} \\ &= \Pr\left\{\operatorname{sgn}\{h_{n,k}^R\} \operatorname{sgn}\left\{ \Re\{h_{n,k} x_k\} + \Re\{w_n\} + \sum_{j \neq k} \Re\{h_{n,j} x_j\} \right\} = 1\right\} \\ &\approx \Phi(\zeta_{1,n}^{RR}), \end{aligned} \quad (20)$$

where in the last step, we have approximated the interference term $\sum_{j \neq k} \Re\{h_{n,j} x_j\}$ as a zero-mean Gaussian random variable with variance $\rho \sum_{j \neq k} |h_{n,j}|^2$ and defined

$$\zeta_{1,n}^{RR} = \sqrt{\frac{2\rho}{1 + \rho \sum_{j \neq k} |h_{n,j}|^2}} \left(\left|h_{n,k}^R\right| x_k^R - \frac{h_{n,k}^I x_k^I}{\operatorname{sgn}\{h_{n,k}^R\}} \right). \quad (21)$$

For the single-user case, the approximation (20) is exact since there is no interference. Proceeding in an analogous way, we can show that $\Pr\left\{c_n^{I,I}=1\right\} \approx \Phi(\zeta_{2,n}^{II})$, that $\Pr\left\{c_n^{R,I}=1\right\} \approx \Phi(\zeta_{1,n}^{R,I})$ and that $\Pr\left\{c_n^{I,R}=1\right\} \approx \Phi(\zeta_{2,n}^{I,R})$, where

$$\zeta_{2,n}^{II} = \sqrt{\frac{2\rho}{1+\rho\sum_{j\neq k}|h_{n,j}|^2}}\left(\left|h_{n,k}^I\right| x_k^R + \frac{h_{n,k}^R x_k^I}{\mathrm{sgn}\{h_{n,k}^I\}}\right) \tag{22}$$

$$\zeta_{1,n}^{R,I} = \sqrt{\frac{2\rho}{1+\rho\sum_{j\neq k}|h_{n,j}|^2}}\left(\left|h_{n,k}^R\right| x_k^I + \frac{h_{n,k}^I x_k^R}{\mathrm{sgn}\{h_{n,k}^R\}}\right) \tag{23}$$

and

$$\zeta_{2,n}^{I,R} = \sqrt{\frac{2\rho}{1+\rho\sum_{j\neq k}|h_{n,j}|^2}}\left(\left|h_{n,k}^I\right| x_k^I - \frac{h_{n,k}^R x_k^R}{\mathrm{sgn}\{h_{n,k}^I\}}\right). \tag{24}$$

Next, we use these approximations to derive $\boldsymbol{\mu}(x_k,\hat{\mathbf{H}})$ and $\Sigma(x_k,\hat{\mathbf{H}})$.

1) MRC receiver: It follows from (10) and (16) that the receive filter for the kth user can be written as $\mathbf{a}_k = \frac{1}{2N}\left(\mathrm{sgn}\{\Re\{\mathbf{h}_k\}\} + j\mathrm{sgn}\{\Im\{\mathbf{h}_k\}\}\right)$. Consequently, the real and imaginary components of $\hat{x}_k$ reduce to

$$\hat{x}_k^R = \frac{1}{2N}\sum_{n=1}^{N}\left(\mathrm{sgn}\{h_{n,k}^R\}\, r_n^R + \mathrm{sgn}\{h_{n,k}^I\}\, r_n^I\right) = \frac{1}{2N}\sum_{n=1}^{N}\left(c_n^{R,R} + c_n^{I,I}\right) \tag{25}$$

and

$$\hat{x}_k^I = \frac{1}{2N}\sum_{n=1}^{N}\left(\mathrm{sgn}\{h_{n,k}^R\}\, r_n^I - \mathrm{sgn}\{h_{n,k}^I\}\, r_n^R\right) = \frac{1}{2N}\sum_{n=1}^{N}\left(c_n^{R,I} - c_n^{I,R}\right). \tag{26}$$

For the real component, we note that $(c_n^{R,R}+c_n^{I,I})$ is supported on $\{-2,0,2\}$ and that $\Pr\{(c_n^{R,R}+c_n^{I,I})=-2\} = \Phi(-\zeta_{1,n}^{RR})\Phi(-\zeta_{2,n}^{II})$ and $\Pr\{(c_n^{R,R}+c_n^{I,I})=2\} = \Phi(\zeta_{1,n}^{RR})\Phi(\zeta_{2,n}^{II})$. Thus, the conditional mean of $\hat{x}_k^R$ given x_k and $\hat{\mathbf{H}}$, can be written as

$$\begin{aligned}
\mathbb{E}\left[\hat{x}_k^R \,|\, x_k, \hat{\mathbf{H}}\right] &= \frac{1}{2N}\sum_{n=1}^{N}\mathbb{E}\left[c_n^{R,R}+c_n^{I,I}\right] \\
&= \frac{1}{N}\sum_{n=1}^{N}\left(\Phi(\zeta_{1,n}^{RR})\Phi(\zeta_{2,n}^{II}) - \Phi(-\zeta_{1,n}^{RR})\Phi(-\zeta_{2,n}^{II})\right) \\
&= \frac{1}{N}\sum_{n=1}^{N}\left(\Phi(\zeta_{1,n}^{RR}) - \Phi(-\zeta_{2,n}^{II})\right).
\end{aligned} \tag{27}$$

Similarly, for the imaginary part, it holds that

$$\mathbb{E}\left[\hat{x}_k^I \,|\, x_k, \hat{\mathbf{H}}\right] = \frac{1}{N}\sum_{n=1}^{N}\left(\Phi(\zeta_{1,n}^{R,I}) - \Phi(-\zeta_{2,n}^{I,R})\right). \tag{28}$$

The sought-after mean vector is then

$$\boldsymbol{\mu}(x_k, \mathbf{H}) = \frac{1}{N} \sum_{n=1}^{N} \begin{bmatrix} \Phi(\zeta_{1,n}^{RR}) - \Phi(-\zeta_{2,n}^{II}) \\ \Phi(\zeta_{1,n}^{R,I}) - \Phi(-\zeta_{2,n}^{I,R}) \end{bmatrix}. \tag{29}$$

Moving to $\Sigma(x_k, \mathbf{H})$, its first entry can be obtained as follows

$$\begin{aligned} [\Sigma(x_k, \mathbf{H})]_{1,1} &= \mathbb{E}\Big[\big(\hat{x}_k^R\big)^2 \mid x_k, \hat{\mathbf{H}}\Big] - \mathbb{E}\Big[\hat{x}_k^R \mid x_k, \hat{\mathbf{H}}\Big]^2 \\ &= \frac{1}{N^2} \sum_{n=1}^{N} \Big(\Phi(\zeta_{1,n}^{RR})\Phi(\zeta_{2,n}^{II}) + \Phi(-\zeta_{1,n}^{RR})\Phi(-\zeta_{2,n}^{II}) - \big(\Phi(\zeta_{1,n}^{RR}) - \Phi(-\zeta_{2,n}^{II})\big)^2\Big) \\ &= \frac{1}{N^2} \sum_{n=1}^{N} \left(\Phi(\zeta_{1,n}^{RR})\Phi(-\zeta_{1,n}^{RR}) + \Phi(\zeta_{2,n}^{II})\Phi(-\zeta_{2,n}^{II})\right). \end{aligned} \tag{30}$$

Analogously, it holds that

$$\begin{aligned} [\Sigma(x_k, \mathbf{H})]_{2,2} &= \mathbb{E}\Big[\big(\hat{x}_k^I\big)^2 \mid x_k, \hat{\mathbf{H}}\Big] - \mathbb{E}\Big[\hat{x}_k^I \mid x_k, \hat{\mathbf{H}}\Big]^2 \\ &= \frac{1}{N^2} \sum_{n=1}^{N} \Big(\Phi(\zeta_{1,n}^{R,I})\Phi(-\zeta_{1,n}^{R,I}) + \Phi(\zeta_{2,n}^{I,R})\Phi(-\zeta_{2,n}^{I,R})\Big). \end{aligned} \tag{31}$$

Furthermore, it can be verified that $\left(c_n^{R,R} + c_n^{I,I}\right)\left(c_n^{R,I} - c_n^{I,R}\right) = 0$, which means that we can write

$$\begin{aligned} [\Sigma(x_k, \mathbf{H})]_{1,2} &= \mathbb{E}\Big[\hat{x}_k^R \hat{x}_k^I \mid x_k, \hat{\mathbf{H}}\Big] - \mathbb{E}\Big[\hat{x}_k^R \mid x_k, \hat{\mathbf{H}}\Big]\,\mathbb{E}\Big[\hat{x}_k^I \mid x_k, \hat{\mathbf{H}}\Big] \\ &= \frac{1}{N^2} \sum_{n=1}^{N} \left(\mathbb{E}\left[\left(c_n^{R,R} + c_n^{I,I}\right)\left(c_n^{R,I} - c_n^{I,R}\right)\right] - \mathbb{E}\left[c_n^{R,R} + c_n^{I,I}\right]\mathbb{E}\left[c_n^{R,I} + c_n^{I,R}\right]\right) \\ &= -\frac{1}{N^2} \sum_{n=1}^{N} \mathbb{E}\left[c_n^{R,R} + c_n^{I,I}\right]\mathbb{E}\left[c_n^{R,I} + c_n^{I,R}\right] \\ &= -\frac{1}{N^2} \sum_{n=1}^{N} \left(\Phi(\zeta_{1,n}^{RR}) - \Phi(-\zeta_{2,n}^{II})\right)\Big(\Phi(\zeta_{1,n}^{R,I}) - \Phi(-\zeta_{2,n}^{I,R})\Big). \end{aligned} \tag{32}$$

Finally, because of symmetry,

$$[\Sigma(x_k, \mathbf{H})]_{2,1} = [\Sigma(x_k, \mathbf{H})]_{1,2}. \tag{33}$$

2) ZF receiver: For the ZF receiver, we resort to (17) and (18) to derive the required mean vector. In this case, $(c_n^{R,R} + c_n^{I,I})$ and $(c_n^{R,I} - c_n^{I,R})$ are quaternary random variables. Following the same steps as for the MRC receiver, the mean can be written as follows:

$$\boldsymbol{\mu}(x_k, \mathbf{H}) = \sum_{n=1}^{N} \begin{bmatrix} 2\Big(\frac{a_{n,k}^R}{\mathrm{sgn}\{h_{n,k}^R\}}\Phi(\zeta_{1,n}^{RR}) - \frac{a_{n,k}^I}{\mathrm{sgn}\{h_{n,k}^I\}}\Phi(-\zeta_{2,n}^{II})\Big) - \frac{a_{n,k}^R}{\mathrm{sgn}\{h_{n,k}^R\}} - \frac{a_{n,k}^I}{\mathrm{sgn}\{h_{n,k}^I\}} \\ 2\Big(\frac{a_{n,k}^R}{\mathrm{sgn}\{h_{n,k}^R\}}\Phi(\zeta_{1,n}^{R,I}) - \frac{a_{n,k}^I}{\mathrm{sgn}\{h_{n,k}^I\}}\Phi(-\zeta_{2,n}^{I,R})\Big) - \frac{a_{n,k}^R}{\mathrm{sgn}\{h_{n,k}^R\}} - \frac{a_{n,k}^I}{\mathrm{sgn}\{h_{n,k}^I\}} \end{bmatrix}. \tag{34}$$

For the ZF receiver, the assumption that the interference is uncorrelated across the receive antennas does not yield a satisfactory approximation. Therefore, we resort to Monte-Carlo simulations to obtain the covariance.

ACKNOWLEDGEMENTS

The authors would like to thank Dr. Fredrik Athley at Ericsson Research for fruitful discussions.

REFERENCES

[1] S. Jacobsson, G. Durisi, M. Coldrey, U. Gustavsson, and C. Studer, "One-bit massive MIMO: Channel estimation and high-order modulations," in *Proc. IEEE Int. Conf. Commun. (ICC)*, London, U.K., June 2015, pp. 1304–1309.

[2] E. G. Larsson, F. Tufvesson, O. Edfors, and T. L. Marzetta, "Massive MIMO for next generation wireless systems," *IEEE Commun. Mag.*, vol. 52, no. 2, pp. 186–195, Feb. 2014.

[3] T. L. Marzetta, "Noncooperative cellular wireless with unlimited numbers of base station antennas," *IEEE Trans. Wireless Commun.*, vol. 9, no. 11, pp. 3590–3600, Nov. 2010.

[4] H. Yang and T. L. Marzetta, "Total energy efficiency of cellular large scale antenna system multiple access mobile networks," in *Proc. IEEE Online Conf. Green Commun. (OnlineGreenComm)*, Piscataway, NJ, Oct. 2013, pp. 27–32.

[5] U. Gustavsson, C. Sanchéz-Perez, T. Eriksson, F. Athley, G. Durisi, P. Landin, K. Hausmair, C. Fager, and L. Svensson, "On the impact of hardware impairments on massive MIMO," in *Proc. IEEE Global Telecommun. Conf. (GLOBECOM)*, Austin, TX, Dec. 2014, pp. 294–300.

[6] X. Zhang, M. Matthaiou, E. Björnson, M. Coldrey, and M. Debbah, "On the MIMO capacity with residual transceiver hardware impairments," in *Proc. IEEE Int. Conf. Commun. (ICC)*, Sydney, Australia, Jun. 2014, pp. 5299–5305.

[7] E. Björnson, J. Hoydis, M. Kountouris, and M. Debbah, "Massive MIMO systems with non-ideal hardware: Energy efficiency, estimation, and capacity limits," *IEEE Trans. Inf. Theory*, vol. 11, no. 60, pp. 7112–7139, Nov. 2014.

[8] R. H. Walden, "Analog-to-digital converter survey and analysis," *IEEE J. Sel. Areas Commun.*, vol. 17, no. 4, pp. 539–550, Apr. 1999.

[9] B. Murmann, "ADC performance survey 1997-2015." [Online]. Available: http://web.stanford.edu/~murmann/adcsurvey.html

[10] Ericsson AB, Huawei Technologies, NEC Corporation, Alcatel Lucent, and Nokia Siemens Networks, *Common public radio interface (CPRI); Interface Specification*, CPRI specification v6.0, Aug. 2013.

[11] S.-H. Park, O. Simeone, O. Sahin, and S. Shamai (Shitz), "Fronthaul compression for cloud radio access networks," *IEEE Signal Process. Mag.*, vol. 31, no. 6, pp. 69–79, Nov. 2014.

[12] I. D. O'Donnell and R. W. Brodersen, "An ultra-wideband transceiver architecture for low power, low rate, wireless systems," *IEEE Trans. Veh. Technol.*, vol. 54, no. 5, pp. 1623–1631, Sep. 2005.

[13] S. Hoyos, B. M. Sadler, and G. R. Arce, "Monobit digital receivers for ultrawideband communications," *IEEE Trans. Wireless Commun.*, vol. 4, no. 4, pp. 1337–1344, Jul. 2005.

[14] J. Singh, O. Dabeer, and U. Madhow, "On the limits of communication with low-precision analog-to-digital conversion at the receiver," *IEEE Trans. Commun.*, vol. 57, no. 12, pp. 3629–3639, Dec. 2009.

[15] T. Koch and A. Lapidoth, "At low SNR, asymmetric quantizers are better," *IEEE Trans. Inf. Theory*, vol. 59, no. 9, pp. 5421–5445, Sep. 2013.

[16] S. Verdú, "Spectral efficiency in the wideband regime," *IEEE Trans. Inf. Theory*, vol. 48, no. 6, pp. 1319–1343, Jun. 2002.

[17] S. Krone and G. Fettweis, "Fading channels with 1-bit output quantization: Optimal modulation, ergodic capacity and outage probability," in *IEEE Inf. Theory Workshop (ITW)*, Dublin, Ireland, Aug. 2010.

[18] A. Mezghani and J. A. Nossek, "Analysis of Rayleigh-fading channels with 1-bit quantized output," in *Proc. IEEE Int. Symp. Inf. Theory (ISIT)*, Toronto, ON, Jul. 2008, pp. 260–264.

[19] ——, "On ultra-wideband MIMO systems with 1-bit quantized outputs: Performance analysis and input optimization," in *Proc. IEEE Int. Symp. Inf. Theory (ISIT)*, Nice, France, Jun. 2007, pp. 1286–1289.

[20] J. Mo and R. W. Heath Jr., "Capacity analysis of one-bit quantized MIMO systems with transmitter channel state information," *IEEE Trans. Signal Process.*, vol. 63, no. 20, pp. 5498–5512, Oct 2015.

[21] T. M. Lok and V. K.-W. Wei, "Channel estimation with quantized observations," in *Proc. IEEE Int. Symp. Inf. Theory (ISIT)*, Cambridge, MA, Aug. 1998, p. 333.

[22] M. T. Ivrlac and J. A. Nossek, "On MIMO channel estimation with single-bit quantization," in *Int. ITG Workshop on Smart Antennas (WSA)*, Vienna, Austria, Feb. 2007.

[23] A. Zymnis, S. Boyd, and E. Candès, "Compressed sensing with quantized measurements," *IEEE Signal Process. Lett.*, vol. 17, no. 2, pp. 149–152, Feb. 2010.

[24] C. Risi, D. Persson, and E. G. Larsson, "Massive MIMO with 1-bit ADC," Apr. 2014. [Online]. Available: http://arxiv.org/abs/1404.7736

[25] J. Choi, J. Mo, and R. W. Heath Jr., "Near maximum-likelihood detector and channel estimator for uplink multiuser massive MIMO systems with one-bit ADCs," vol. 64, no. 5, pp. 2005–2018, May 2016.

[26] N. Liang and W. Zhang, "Mixed-ADC massive MIMO," *IEEE J. Sel. Areas Commun.*, vol. 34, no. 4, pp. 983–997, May 2016.

[27] S. Wang, Y. Li, and J. Wang, "Multiuser detection in massive spatial modulation MIMO with low-resolution ADCs," *IEEE Trans. Wireless Commun.*, pp. 2156–2168, Dec. 2014.

[28] C. Studer and G. Durisi, "Quantized massive MU-MIMO-OFDM uplink," *IEEE Trans. Commun.*, vol. 64, no. 6, pp. 2387–2399, Jun. 2016.

[29] S. Shamai (Shitz), "Information rates by oversampling the sign of a bandlimited process," *IEEE Trans. Inf. Theory*, vol. 40, no. 4, pp. 1230–1236, Jul. 1994.

[30] T. Koch and A. Lapidoth, "Increased capacity per unit-cost by oversampling," in *Proc. IEEE 26th Conv. Electrical and Electronics Engineers in Israel (IEEEI)*, Eliat, Israel, Nov. 2010, pp. 684–688.

[31] S. Krone and G. Fettweis, "Capacity of communications channels with 1-bit quantization and oversampling at the receiver," in *Proc. IEEE Sarnoff Symp. (SARNOFF)*, Newark, NJ, May 2012.

[32] T. L. Marzetta and B. M. Hochwald, "Capacity of a mobile multiple-antenna communication link in Rayleigh flat fading," *IEEE Trans. Inf. Theory*, vol. 45, no. 1, pp. 139–157, Jan. 1999.

[33] A. Lapidoth, "On the asymptotic capacity of stationary Gaussian fading channels," *IEEE Trans. Inf. Theory*, vol. 51, no. 2, pp. 437–446, Feb. 2005.

[34] G. Durisi, T. Koch, J. Östman, Y. Polyanskiy, and W. Yang, "Short-packet communications over multiple-antenna Rayleigh-fading channels," vol. 64, no. 2, pp. 618–629, Feb. 2016.

[35] W. Yang, G. Durisi, and E. Riegler, "On the capacity of large-MIMO block-fading channels," *IEEE J. Sel. Areas Commun.*, vol. 31, no. 2, pp. 117–132, Feb. 2013.

[36] R. Devassy, G. Durisi, J. Östman, W. Yang, T. Eftimov, and Z. Utkovski, "Finite-SNR bounds on the sum-rate capacity of Rayleigh block-fading multiple-access channels with no a priori CSI," *IEEE Trans. Commun.*, vol. 63, no. 10, pp. 3621–3632, Oct. 2015.

[37] S. Jacobsson, “Throughput analysis of massive MIMO uplink with one-bit ADCs,” Master’s thesis, Chalmers University of Technology, 2015.

[38] C.-K. Wen, S. Jin, K.-K. Wong, C.-J. Wang, and G. Wu, “Joint channel-and-data estimation for large-MIMO systems with low-precision ADCs,” in *Proc. IEEE Int. Symp. Inf. Theory (ISIT)*, Hong Kong, Jun. 2015, pp. 1237–1241.

[39] E. Björnson, E. G. Larsson, and T. L. Marzetta, “Massive MIMO: 10 myths and one critical question,” *IEEE Commun. Mag.*, vol. 54, no. 2, pp. 114–123, Aug. 2016.

[40] R. M. Gray and T. G. Stockham Jr., “Dithered quantizers,” *IEEE Trans. Inf. Theory*, vol. 39, no. 3, pp. 805–812, May 1993.

[41] O. Dabeer and A. Karnik, “Signal parameter estimation using 1-bit dithered quantization,” *IEEE Trans. Inf. Theory*, vol. 52, no. 12, pp. 5389–5405, Dec. 2006.

[42] G. Zeitler, G. Kramer, and A. C. Singer, “Bayesian parameter estimation using single-bit dithered quantization,” *IEEE Trans. Signal Process.*, vol. 60, no. 6, pp. 2713–2726, Jun. 2012.

[43] L. Tong, B. M. Sadler, and M. Dong, “Pilot-assisted wireless transmissions: general model, design criteria, and signal processing,” *IEEE Signal Process. Mag.*, vol. 21, no. 6, pp. 12–25, Nov. 2004.

[44] D. M. Arnold, H.-A. Loeliger, P. O. Vontobel, A. Kavcic, and W. Zeng, “Simulation-based computation of information rates for channels with memory,” *IEEE Trans. Inf. Theory*, vol. 52, no. 8, pp. 3498–3508, Aug. 2006.

[45] T. M. Cover and J. A. Thomas, *Elements of Information Theory*, 2nd ed., 2006.

[46] J. Max, “Quantizing for minimum distortion,” *IRE Trans. Inf. Theory*, vol. 6, no. 1, pp. 7–12, Mar. 1960.

[47] S. P. Lloyd, “Least squares quantization in PCM,” *IEEE Trans. Inf. Theory*, vol. 28, no. 2, pp. 129–137, Mar. 1982.

[48] 3GPP, “Spatial channel model for multiple input multiple output (MIMO) simulations,” Tech. Rep. 25.996 ver. 12.0.0 rel. 12, Sep. 2014.